

Deposition and mobilization of clay colloids in unsaturated porous media

Bin Gao and James E. Saiers

School of Forestry and Environmental Studies, Yale University, New Haven, Connecticut, USA

Joseph N. Ryan

Department of Civil, Environmental, and Architectural Engineering, University of Colorado, Boulder, Colorado, USA

Received 16 March 2004; revised 7 June 2004; accepted 22 June 2004; published 28 August 2004.

[1] We report results on the effects of porewater pH and transients in porewater flow on the deposition and mobilization of colloid-sized clay particles within unsaturated sand columns. The deposition rates of illite under steady-flow conditions were essentially independent of pH, while the deposition rates of kaolinite nearly doubled as the pH decreased from 7.4 to 4.6. Mobilization of kaolinite colloids was slow or negligible under steady-flow conditions; however, transients in porewater flow induced rapid colloid release. A model that accounts for rate-limited deposition reactions and that links colloid mobilization to variations in moisture content and porewater velocity describes the effluent colloid concentrations measured during the steady-flow and transient-flow stages of the column experiments. On the basis of these results we infer that the effects of pH on clay-colloid deposition depend on the mineralogy of the clay colloids and that perturbations in flow are critical in mobilizing clay colloids within the vadose zone. **INDEX TERMS:** 1875 Hydrology: Unsaturated zone; 1866 Hydrology: Soil moisture; 1806 Hydrology: Chemistry of fresh water; **KEYWORDS:** colloids, colloid deposition, colloid mobilization, clay particles, vadose zone

Citation: Gao, B., J. E. Saiers, and J. N. Ryan (2004), Deposition and mobilization of clay colloids in unsaturated porous media, *Water Resour. Res.*, 40, W08602, doi:10.1029/2004WR003189.

1. Introduction

[2] Vadose zone environments typically contain colloid-sized clay particles in great abundance [Denovio *et al.*, 2004]. These clay colloids can adsorb a variety of contaminants and, if mobilized, may carry contaminants across the water table and into groundwater aquifers [Ryan *et al.*, 1998; Sprague *et al.*, 2000]. Colloid mobilization occurs during infiltration events that are characterized by spatio-temporal changes in porewater flow rate, moisture content, and porewater chemistry [Pilgrim and Huff, 1983; El-Farhan *et al.*, 2000; Saiers *et al.*, 2003; Rousseau *et al.*, 2004]. Once mobilized, colloids travel by advection and dispersion and can be removed from the porewater by reactions that take place at solid-water and air-water interfaces [Wan and Wilson, 1994; Gamedainger and Kaplan, 2001; Cherrey *et al.*, 2003]. The rates of the deposition reactions vary broadly and depend on the physicochemical properties of the soil-water-colloid system [Wan and Tokunaga, 1997; Lenhart and Saiers, 2002; Saiers and Lenhart, 2003].

[3] In this work, we describe results from column experiments and model simulations that are designed to address four questions related to the controls on clay-colloid movement through unsaturated porous media: (1) How do the deposition kinetics of clay colloids respond to variations in porewater pH? (2) Does the relationship between pH and

deposition rates vary as a function of clay-colloid mineralogy? (3) How does clay-colloid retention differ between saturated media, where colloid deposition occurs only at solid-water interfaces, and unsaturated media, where colloids collect at both solid-water and air-water interfaces? (4) What effects do perturbations in volumetric moisture content have on the mobilization of clay colloids? To our knowledge, these questions have not been addressed before in the context of clay-colloid transport in unsaturated porous media. The answers to these questions should illuminate how key variables that characterize the vadose zone affect the movement of clay colloids and should improve conceptual and theoretical descriptions of the processes of colloid-facilitated contaminant transport and soil-profile development.

2. Experimental Methods

2.1. Preparation of Colloidal Suspensions

[4] Kaolinite (EM Science) was purchased as a powder and illite (Clay Minerals Society) was obtained as an aggregate and pulverized with an agate mortar and pestle. One gram of the clay powder (kaolinite or illite) was suspended in a solution of pH 4.6, 6.0, or 7.4 that was adjusted to an ionic strength of 0.001 M by the addition of NaCl. (The low ionic strength of this water is typical of near-surface soil waters, and the endpoints of this pH range bracket the pH of soil solutions collected from around the world [Sparks, 1995]). The clay suspension was shaken vigorously, placed in an ultrasonic bath for 30 minutes, and

Table 1. Electrophoretic Mobility (EM) and Zeta Potential (ξ) of the Quartz Sand and Clay Colloids

pH	Quartz		Kaolinite		Illite	
	EM, $10^{-8} \text{ m}^2 \text{ s}^{-1} \text{ V}^{-1}$	ξ , mV	EM, $10^{-8} \text{ m}^2 \text{ s}^{-1} \text{ V}^{-1}$	ξ , mV	EM, $10^{-8} \text{ m}^2 \text{ s}^{-1} \text{ V}^{-1}$	ξ , mV
7.4	-4.26	-57.65	-3.21	-43.42	-3.08	-41.68
6.0	-3.96	-52.63	-2.85	-38.61	-3.02	-40.97
4.6	-3.45	-46.7	-2.35	-31.88	-2.49	-33.76

let stand for 24 hours. The fraction of clay colloids remaining in suspension was siphoned into a second flask, and the concentration of colloids in an aliquot of this stock suspension was determined gravimetrically before diluting the stock to a colloid concentration of 100 mg L^{-1} with a pH-matched electrolyte solution. The mean sizes of the clay colloids, as determined by photon correlation spectroscopy, did not vary significantly with pH and equaled $0.30 \text{ }\mu\text{m}$ for kaolinite and $0.26 \text{ }\mu\text{m}$ for illite. The zeta potentials of the clay colloids and quartz sand, calculated from measurements of electrophoretic mobility, were negative in sign and decreased in magnitude with decreasing pH (Table 1).

2.2. Column Design and Instrumentation

[5] For each experiment, fresh sand (355 to $425 \text{ }\mu\text{m}$), cleaned according to the procedures reported by *Lenhart and Saiers* [2002], was wet-packed in an acrylic column measuring 12.7 cm in diameter and 32.8 cm in length. The porosity of the sand pack equaled 0.34 . Probes for measuring volumetric moisture content (Θ) and tensionmeters for measuring capillary pressure head (Ψ) were inserted at 7.7 , 16.4 , and 25.1 cm from the top of the column. Data from the moisture probes and tensionmeters were recorded with a data logger. Peristaltic pumps at the column inlet and outlet regulated the sand-pack moisture content and controlled the downward flow of water and colloids through the column. Additional details on column construction and instrumentation are provided by *Lenhart and Saiers* [2002].

2.3. Column Experiments

[6] To prepare for an unsaturated transport experiment, the sand column was drained to a moisture content of 0.12 by elevating the outflow rate to $70 \text{ cm}^3 \text{ h}^{-1}$ above the inflow rate of colloid-free water. The colloid-free water was adjusted to pH 4.6 , 6.0 , or 7.4 . Approximately 12 h were required to reach the target moisture content, whereupon a unit hydraulic head gradient was established throughout the sand pack by equalizing the inflow and outflow rates. The average linear porewater velocity (v) under steady and uniform flow equaled 0.66 cm min^{-1} .

[7] Once the column moisture content stabilized at 0.12 and the effluent pH matched the influent pH (4.6 , 6.0 , or 7.4), a 100 mg L^{-1} clay-colloid suspension was introduced to the top of the column for 3 h . Following application of the colloid pulse, the column was flushed without perturbing the flow rate with a colloid-free water of the same pH as the clay-particle suspension. Water samples were collected from base of the column with a fraction collector during colloid injection and column flushing and analyzed for colloid concentrations by measuring the total extinction of light at a wavelength of 350 nm with a UV-visible spectrophotometer. Colloids not eluted from the column during the steady-flow flush were assumed to be captured by air-water

interfaces, attached to the sand grains, or strained within narrow porewater conduits that lined partially saturated pores.

[8] The steady-flow period in the experiments with kaolinite was followed by a transient-flow stage in which the mobilization of previously retained kaolinite was measured in response to increases in specific discharge (q) and corresponding increases in Θ . This involved increasing q in three steps from 0.08 cm min^{-1} (i.e., the q during colloid application) to 0.16 , 0.32 , and finally to 0.55 cm min^{-1} . The average linear porewater velocity ($v = q/\Theta$) at the end of the transient-flow stage equaled 2.9 cm min^{-1} , 4.4 times greater than the v during the steady-flow stage of the experiments when the kaolinite colloids were applied to the column.

[9] The transport of both kaolinite and illite colloids also was measured in water-saturated sand ($\Theta = 0.34$) under steady-flow conditions at pH 4.6 , 6.0 , and 7.4 . The influent concentrations of colloids used in these experiments equaled 100 mg L^{-1} , and v equaled 0.66 cm min^{-1} , matching that of the unsaturated experiments. Following the steady-flow stage in the pH 4.6 experiments with kaolinite, v was increased in a single step from 0.66 to 2.64 cm min^{-1} to examine the effects of flow rate increases on colloid mobilization.

3. Model for Mobilization, Transport, and Deposition

[10] Here we summarize a published model [*Saiers and Lenhart*, 2002] that can be used as a diagnostic tool to quantify the rates of colloid deposition in the experiments and to test expectations about relationships between porewater flow transients and colloid mobilization. The model solves the advection-dispersion equation for the transport of the clay colloids:

$$\frac{\partial(\Theta C)}{\partial t} + \rho_b \frac{\partial \Gamma_{STR}}{\partial t} + \frac{\partial((1-\Theta)\Gamma_{TIR})}{\partial t} = \frac{\partial}{\partial z} \left[D\Theta \frac{\partial C}{\partial z} \right] - \frac{\partial(qC)}{\partial z} \quad (1)$$

where C is the porewater colloid concentration, Γ_{STR} is the concentration of colloids immobilized by straining (colloid mass per sand mass), Γ_{TIR} is the sum of the concentrations of colloids immobilized by air-water interface capture and sand grain attachment (colloid mass per volume of air and sand), ρ_b is the bulk density, Θ is the volumetric moisture content, D is the dispersion coefficient, q is the specific discharge, t is time, and z is the coordinate parallel to flow. Variations in q and Θ , which were induced in our experiments through adjustment of the column inflow and outflow rates, are specified on the basis of the numerical solution to the Richards equation. Equation (1) is coupled

with equations for the rate-limited transfer of colloids between mobile and immobile phases.

[11] Immobilization by straining occurs within porewater conduits that are too narrow to permit the colloids to pass [Wan and Tokunaga, 1997]. The submicrometer clay colloids are too small to be strained within the water-saturated pore spaces of our sand pack, but may become trapped at the three-phase contacts of pore-corner menisci, within adsorbed water films, and at the termini of discontinuous porewater ducts. The release of strained colloids is negligible during steady porewater flow; however, increases in Θ promote expansion of porewater conduits, which leads to mobilization. Observations on the mobilization of strained silica colloids during porous medium imbibition (wetting) reveal that the fraction of colloids eligible for release increases with increasing Θ [Saiers and Lenhart, 2002]. This finding suggests that dimensions of the porewater conduits exhibit a distributed response to changes in measured Θ , which spreads colloid release over a range of Θ .

[12] A phenomenological way to distribute colloid mobilization during the imbibition process is to divide the population of strained colloids into a series of compartments that release colloids at different moisture contents [Saiers and Lenhart, 2002]. We assume that a first-order rate law describes the temporal change in the concentration of strained colloids within the i th compartment, such that

$$\frac{\partial \Gamma_{STR_i}}{\partial t} = \frac{k_{STR}}{\rho_b N_C} \Theta C - k_{Ri} \Gamma_{STR_i} \quad (2a)$$

while the temporal variation in the total concentration of strained colloids is

$$\frac{\partial \Gamma_{STR}}{\partial t} = \sum_{i=1}^{N_C} \frac{\partial \Gamma_{STR_i}}{\partial t} \quad (2b)$$

where N_C is the number of compartments, k_{STR} is the straining-rate coefficient, and k_{Ri} is the mobilization rate coefficient for the i th compartment. We assume k_{STR} does not vary between compartments and account for the dependence of k_{STR} on Θ and v with an empirical function reported by Lenhart and Saiers [2002]:

$$k_{STR} = \left[1 - \left[\frac{\Theta - \Theta_r}{n - \Theta_r} \right]^{0.6} \right] N_1 v^{0.5} \quad (3)$$

where Θ_r is the residual moisture content, n is porosity, and N_1 is a constant. Values of k_{Ri} vary between compartments according to the relationship between Θ (calculated by solving the Richards equation) and a compartment's characteristic value of critical moisture content:

$$k_{Ri} = 0 \text{ for } \Theta \leq \Theta_{CRi} \quad (4a)$$

$$k_{Ri} = N_2 v \text{ for } \Theta > \Theta_{CRi} \quad (4b)$$

where N_2 is a constant and Θ_{CRi} is the critical moisture content for compartment i . According to equations (4a) and (4b), colloid mobilization from the i th compartment occurs only if Θ exceeds the value of the critical moisture content

assigned to that compartment, in which case k_{Ri} varies directly with v . We treat Θ_{CR} as a continuously distributed variable that can assume any value between Θ_{dep} and n , where Θ_{dep} is the steady state Θ under which colloids were applied to the column ($\Theta_{dep} = 0.12$ in our study). A piecewise linear density function describes the distribution in Θ_{CR} [see Saiers and Lenhart, 2002].

[13] Clay colloids traveling through water-filled pores or relatively large porewater conduits of partially saturated pores are not susceptible to straining, but may diffuse to solid-water or air-water interfaces and be retained by electrostatic forces. We use the terms air-water interface capture and mineral-grain attachment to describe colloid immobilization in cases where electrostatic forces govern colloid adhesion at interfaces. Because the contributions of air-water interface capture and mineral-grain attachment to colloid immobilization cannot be separately resolved (without ambiguity) from analysis of column experiments, we adopt a simple, lumped parameter approach and account for both mechanisms with a single second-order kinetics expression:

$$\frac{\partial((1 - \Theta)\Gamma_{TIR})}{\partial t} = k_{TIR} \left(1 - \frac{\Gamma_{TIR}}{X_{TIR}} \right) \Theta C \quad (5)$$

where k_{TIR} is the rate coefficient for attachment and X_{TIR} is the colloid-retention capacity of the interfaces, which expresses the maximum attainable mass of interface-attached colloids per volume of air and solid. Equation (5) describes an irreversible reaction. Rate laws for irreversible reactions provide a reasonable approximation of air-water interface capture and mineral-grain attachment for conditions of steady porewater flow and chemistry [Saiers and Lenhart, 2003]. During transient-flow, colloids may be mobilized through destruction of air-water interfaces or mobilized from solid-water interfaces by increases in shear or by moving air-water interfaces that scour colloids from the sand-grain surfaces. Equation (5) does not account for these mobilization mechanisms and thus the model presented here will approximate breakthrough concentrations measured during the transient-flow stage of the kaolinite experiments only if the release of strained kaolinite (as described by equations (2a)–(4b)) dominates the mobilization response.

[14] Equations (1)–(5) govern the transport, deposition, and mobilization of colloids in unsaturated and saturated media. These equations for colloid transport and mass transfer, together with the equations for porewater flow (i.e., the Richards equation), were solved numerically by finite differences [Saiers and Lenhart, 2002]. In order to accommodate numerical solution and to be compatible with equations (2a) and (2b), the continuous density for Θ_{CR} must be discretized into N_C compartments. As N_C increases, the discretized form of the Θ_{CR} function converges to the true, continuous form of the density function, which we approximated by setting $N_C = 60$.

4. Model Application Procedures

[15] We quantified colloid deposition in the illite experiments and during the steady-flow stage of the kaolinite experiments by identifying values of k_{STR} , k_{TIR} , and X_{TIR}

that minimized the differences between modeled and measured breakthrough concentrations. The straining rate coefficient (k_{STR}) was set to zero in simulations of clay-colloid transport in saturated sand. Because k_{STR} depends on physical properties, but is independent of porewater chemistry, we used the k_{STR} values estimated from the unsaturated experiments at pH 7.4 to describe straining at pH 6.0 and 4.6.

[16] We quantified mobilization during the transient-flow stage of the kaolinite experiments by adjusting values of N_2 and the shape of the cumulative density for Θ_{CR} in order to obtain a best fit between measured and modeled kaolinite concentrations. The shape of the Θ_{CR} density is governed by the number and position of “anchor” critical moisture contents (Θ_{CR_i}) that separate the straight line segments of the distribution [see *Saiers and Lenhart*, 2002, Figure 1]. The cumulative densities at the anchors, $B(\Theta_{CR_i})$, are found by optimization and the entire distribution is defined through linear interpolation between anchors. We employed the methods described by *Saiers and Lenhart* [2002] to determine the optimal number of anchors and to estimate the cumulative density associated with each anchor.

[17] Colloids mobilized by the transients in Θ and v were susceptible to redeposition deeper within the column. Variations in k_{STR} with Θ and v were described by equation (3). This involved computing N_1 in equation (3) from values of k_{STR} estimated from the steady-flow stage of the experiments and then reapplying the parameterized form of equation (3) to compute k_{STR} variations during transient flow. The parameters k_{TIR} and X_{TIR} likely depend on Θ and v , too, but data are unavailable to define these dependencies. Therefore we used the values of k_{TIR} and X_{TIR} estimated from the steady state stage of the unsaturated experiments to quantify the combined effects of mineral-grain attachment and air-water interface capture on kaolinite immobilization during periods of transient flow. This simplifying assumption should not jeopardize the model descriptions provided that mobilization rates substantially exceed redeposition rates during the transient-flow stage.

5. Experimental Results

5.1. Saturated Experiments

[18] The breakthrough curves on the transport of illite through the saturated sand showed little variation with pH and resembled the breakthrough curve of bromide, a conservative tracer (Figures 1a–1c). The fraction of illite retained within the columns by deposition on the sand grains was very small, ranging from 0.021 at pH 7.4 to 0.029 at pH 4.6. The kaolinite colloids exhibited similarly high mobility in the saturated experiments at pH 6.0 and 7.4 (Figures 1d and 1e); however, effluent concentrations of kaolinite did not exceed 90 mg L^{-1} at pH 4.6 (Figure 1f). A fourfold increase in-flow rate near the end of pH-4.6 experiments failed to mobilize detectable quantities of kaolinite from the quartz sand.

5.2. Steady-Flow Stage of Unsaturated Experiments

[19] Colloid breakthrough was lower in the unsaturated compared to saturated experiments (Figures 2a–2f). The air phase effect was most dramatic with kaolinite at pH 4.6,

where effluent concentrations reached only half the influent levels (Figure 2f). Kaolinite mobility was greater at pH 6.0 and 7.4 and mirrored the mobility of illite, which was about same for the three pH treatments. Nearly 53% of the kaolinite was retained within the unsaturated columns at pH 4.6, compared to 22 to 25% in the remaining unsaturated experiments.

5.3. Transient-Flow Stage of Unsaturated Experiments

[20] In the second stage of the unsaturated experiments with kaolinite, we increased the specific discharge (q) at the column boundaries in three steps from 0.08 to 0.55 cm min^{-1} (Figures 2d–2f). For each change in q , moisture contents measured at 7.7 cm, 16.4 cm, and 25.1 cm from the column top increased by approximately 0.025 and then converged at near-equal values, signaling the reestablishment of uniform flow. Increases in q mobilized kaolinite colloids at concentrations as high as 32 mg L^{-1} . Peak concentrations were highest in the pH-4.6 experiments and, for all three pH treatments, decreased with successive flow perturbations (Figures 2d–2f). Colloid concentrations declined from peak levels shortly after moisture contents restabilized within the column, returning to zero before the onset of the next flow rate perturbation. The flow transients mobilized 19.2, 17.6, and 22.5 mg of kaolinite in experiments at pH 7.4, 6.0, and 4.6, respectively, or nearly half of the kaolinite deposited under steady flow at pH 6.0 and 7.4 and a quarter of the kaolinite deposited under steady flow at pH 4.6 (Table 2).

6. Quantification of Deposition and Mobilization Rates: Application of the Model

6.1. Steady-Flow Stage

[21] The breakthrough curves measured in five of the six experiments conducted in water-saturated media could be closely approximated by adopting the assumption that transport occurred conservatively and by setting k_{TIR} and X_{TIR} to zero (Figures 1a–1e). Both parameters were adjusted in the inverse simulation of kaolinite transport through the saturated sand at pH 4.6 (Table 2), and the good agreement between observed and modeled results suggests equation (5) is appropriate for describing the kinetics of kaolinite deposition onto the sand grains (Figure 1f).

[22] Colloid immobilization by straining in the unsaturated sand is best described by k_{STR} values of 0.17 and 0.18 h^{-1} for illite and kaolinite, respectively. On the basis of these estimates, the timescale for clay-colloid straining (k_{STR}^{-1}) was 6 hours, or about 7 times greater than the timescale for advective transport during the steady-flow stage of the experiments. The kaolinite and illite colloids were similar in size, so the small difference in k_{STR} between the clays is consistent with the notion that straining rates reflect the relationship between colloid size and porewater conduit dimensions.

[23] The parameter k_{TIR} quantifies the initial (clean bed) rates of colloid removal due to air-water interface capture and mineral-grain attachment. Comparison of the best fit values of k_{TIR} determined from the unsaturated experiments to optimal values of k_{STR} shows that electrostatic interactions at “clean” air-water and solid-water interfaces removed colloids faster from porewater than straining

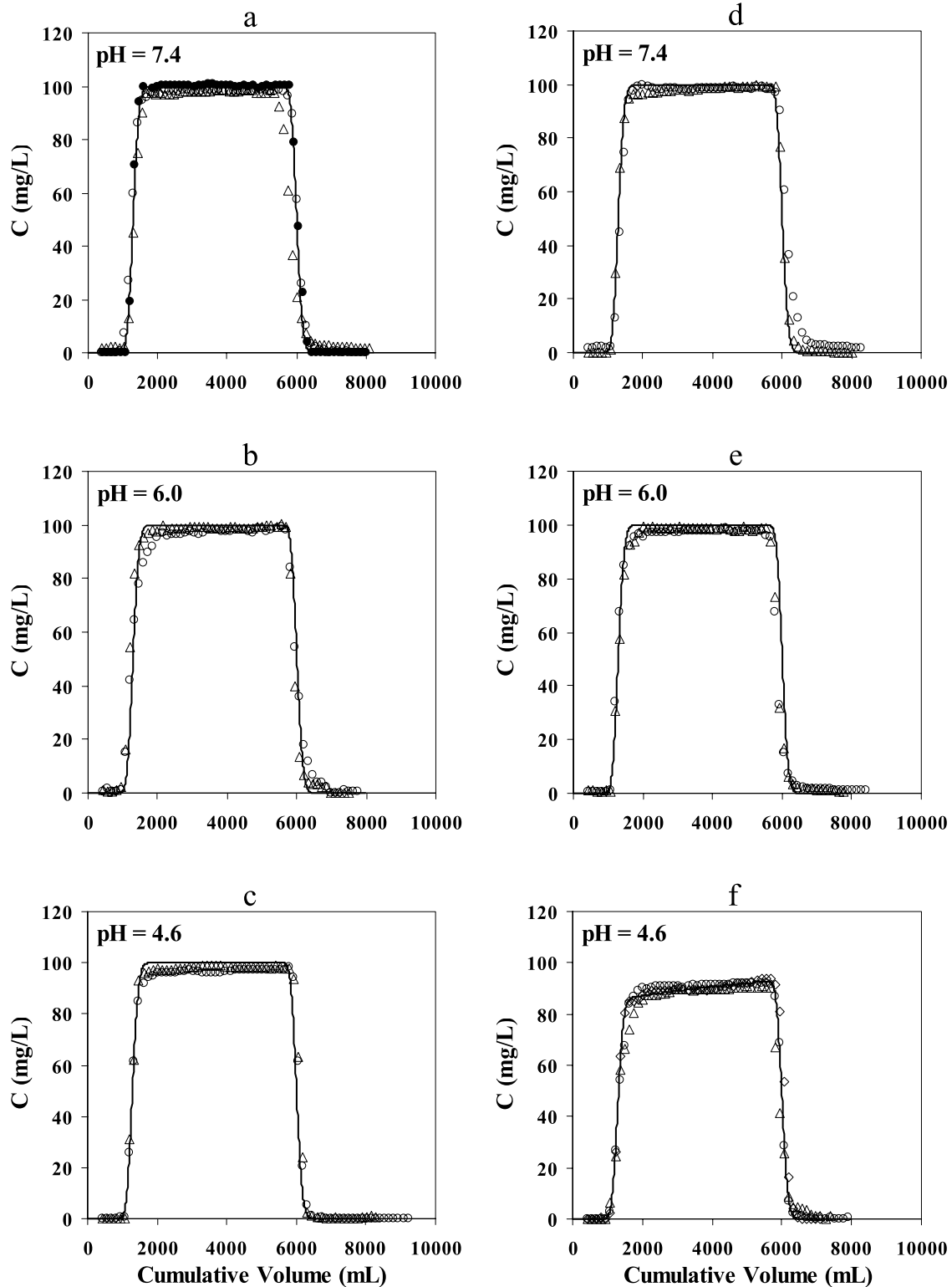


Figure 1. Model-calculated breakthrough curves (lines) and those measured in duplicate experiments (open symbols) for the transport of (a–c) illite and (d–f) kaolinite through water-saturated sand columns. The solid circles in Figure 1a denote breakthrough concentrations of bromide that were measured in a separate experiment.

(Table 2). For the unsaturated experiments with illite, k_{TIR} increases with decreasing porewater pH, but the overall variation across the pH treatments is small. Estimates of k_{TIR} determined for kaolinite fall within the range observed for

illite at pH 6.0 and 7.4. At pH 4.6, k_{TIR} for kaolinite is nearly twice that of illite (Table 2).

[24] The parameter X_{TIR} governs the decline in immobilization rates as colloids collect at the solid-water and air-

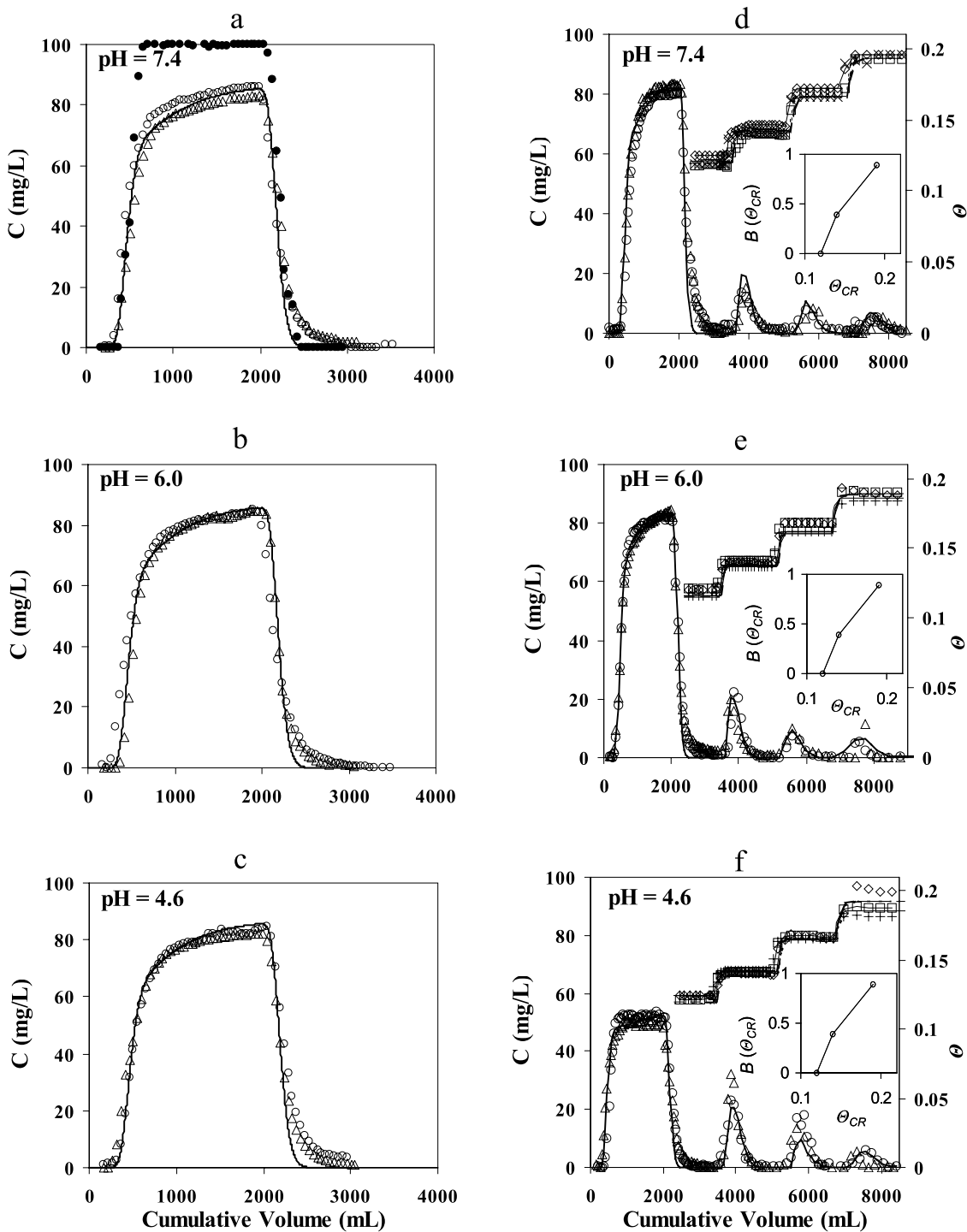


Figure 2. Model-calculated effluent concentrations (lines) and those measured in duplicate experiments (open circles and triangles) with (a–c) illite under steady flow and (d–f) and kaolinite under steady and transient flow. The solid circles in Figure 2a denote the breakthrough curve for bromide. The diamonds, squares, and pluses in Figures 2d–2f delineate moisture contents measured during the transient flow stage at positions 7.7, 16.4, and 25.1 cm from the top of the column, respectively, while the associated lines represent moisture contents computed by solving the Richards equation. The insets in Figures 2d–2f show the optimal cumulative densities for critical moisture content, $B(\theta_{CR})$. The maximum model-computed moisture content ($=0.19$ in our experiments) defines the upper limit for which the θ_{CR} distribution can be reliably estimated, and thus $B(\theta_{CR} = 0.19)$ may be less than unity.

Table 2. Best Fit Parameter Values and Mass Balance Calculations for Experimental Conditions Distinguished on the Basis of pH and Volumetric Moisture Content (Θ) Measured During Steady Flow

Experiment	Colloid Type	pH	Θ	Mass Retained, ^a mg		k_{STR} , h ⁻¹	k_{TIR} , h ⁻¹	X_{TIR} , mg cm ⁻³	N_2 , cm ⁻¹	Mass Mobilized, ^b %
				Strained	Interfaces					
1	kaolinite	4.6	0.12	19.8	71.6	0.18	0.74	1.0×10^{-1}	0.63	24.6
2	kaolinite	6.0	0.12	24.1	16.8	0.18	0.39	4.5×10^{-3}	0.52	42.9
3	kaolinite	7.4	0.12	24.1	17.0	0.18	0.43	4.5×10^{-3}	0.51	46.8
4	illite	4.6	0.12	22.5	15.7	0.17	0.44	4.4×10^{-3}	-	-
5	illite	6.0	0.12	22.6	15.2	0.17	0.42	4.4×10^{-3}	-	-
6	illite	7.4	0.12	22.6	14.9	0.17	0.38	4.3×10^{-3}	-	-
7	kaolinite	4.6	0.34	0	52.0	0	0.19	3.4×10^{-2}	-	0.0
8	kaolinite	6.0	0.34	0	10.8	0	0	0	-	-
9	kaolinite	7.4	0.34	0	11.1	0	0	0	-	-
10	illite	4.6	0.34	0	14.1	0	0	0	-	-
11	illite	6.0	0.34	0	10.2	0	0	0	-	-
12	illite	7.6	0.34	0	10.6	0	0	0	-	-

^aComputed by the mathematical model using best fit parameter values. The subheading ‘‘Strained’’ denotes the colloid mass retained by straining, and the subheading ‘‘Interfaces’’ denotes the colloid mass retained by air- and solid-water interfaces.

^bComputed from the breakthrough data measured during the transient flow stage of experiments.

water interfaces and is a measure of the capacity of these interfaces to retain colloids. Inspection of X_{TIR} values from the unsaturated experiments demonstrates that maximum interfacial coverages of illite were insensitive to pH and less than those for kaolinite, while the capacity of the interfaces to retain kaolinite increased by 22-fold as pH decreased from 6.0 to 4.6 (Table 2).

[25] Model calculations made with the best fit parameter values suggest that straining accounted for greater than 55% of the immobilized colloid mass in all unsaturated experiments, except in the kaolinite experiment conducted at pH 4.6 (Table 2). In this kaolinite experiment, air-water interface capture and mineral-grain attachment dominated retention, accounting for 78% of the immobilized colloid mass. Given that electrostatic forces control clay-colloid adhesion to air-water and solid-water interfaces, these results suggest that the surface charge characteristics of kaolinite were more sensitive to changes in pH than those of illite.

6.2. Transient-Flow Stage

[26] The model reproduces kaolinite concentrations measured during the transient flow stage reasonably well (Figures 2d–2f), suggesting that colloid mobilization was tightly linked to changes in Θ and that the release rate of strained particles increased linearly with v . The parameter N_2 , which relates the mobilization rate coefficient (k_{Ri}) to v , exhibits little variation between pH treatments (Table 2). Calculations made by substituting the N_2 value estimated from the pH-6.0 treatment into equation (4b) show that mobilization rates varied from 35 h⁻¹ after the first flow increase to $v = 1.1$ cm min⁻¹ to 91 h⁻¹ after the last flow increase to $v = 2.9$ cm min⁻¹. The optimal cumulative distributions for Θ_{CR} are nearly identical for the three pH treatments and are characterized by a simple shape and two adjustable anchors (insets in Figures 2d–2f). Low Θ_{CR} values received the greatest weight in these distributions such that 45% of the cumulative density was associated with Θ_{CR} values less than or equal to 0.145 (i.e., $B(0.145) = 0.45$). This indicates that an increase in Θ from 0.12 to 0.145 liberated 45% of the strained colloids, while a comparatively larger change in Θ , from 0.145 to

0.19, was needed to release an additional 45% of the strained colloids.

7. Discussion

[27] We find that initial adhesion rates of illite to air-water and solid-water interfaces (as quantified by k_{TIR}) and the maximum interfacial coverages (as quantified by X_{TIR}) of illite vary weakly with pH. Values of k_{TIR} and X_{TIR} for kaolinite are roughly the same as those for illite at pH 6.0 and 7.4, but are substantially greater at pH 4.6. *Wan and Tokunaga* [2002] measured clay-colloid partitioning in a bubble column and similarly observed that kaolinite partitioning to air-water interfaces was more sensitive to pH changes than that of illite. Kaolinite adhesion to negatively charged air-water and solid-water interfaces is sensitive to pH because it has edge sites that become more protonated (and positively charged) as pH decreases [*Langmuir*, 1997]. Illite also has edge sites with pH-dependent charge, but compared to kaolinite, it has a higher permanent charge, higher aspect ratio, fewer planar edge sites, and a lower zero point of charge [*Wan and Tokunaga*, 2002]. These characteristics dampen the influence of pH on illite adhesion.

[28] The variation in the response of clay-colloid mobility to changes in Θ is attributable to differences in colloid affinities for the air-water and solid-water interfaces. Examination of the best fit values of X_{TIR} estimated from the saturated and unsaturated experiments indicates that the air-water and solid-water interfaces had a relatively low capacity for binding illite at pH 4.6–7.4 and kaolinite at pH 6.0 and 7.4. For these combinations of pH and colloids, straining in partially saturated pores represented the main contributor to immobilization in unsaturated media, and a decrease in Θ from 0.34 to 0.12 led to only a modest (15 mg L⁻¹) decline in peak breakthrough concentrations. Both solid-water and air-water interfaces were more effective in retaining kaolinite at pH 4.6, and calculations based on estimates of X_{TIR} taken from both the saturated and unsaturated experiments reveal that a unit volume of air was capable of immobilizing nearly 9 times more kaolinite than a unit volume of sand at pH 4.6.

Because of the high capacity of air-water interfaces to retain kaolinite at pH 4.6, kaolinite mobility declined precipitously with the transition from saturated to unsaturated conditions.

[29] Transients in flow mobilized kaolinite colloids that were retained within the column under steady-flow conditions. A parametrically simple model that links mobilization to moisture content changes and flow velocity describes the kaolinite concentrations measured during the transient-flow stage with reasonably good success. The largest model data discrepancy occurs in the pH-4.6 experiment where the model underestimates peak effluent concentrations (Figure 2f). Our model accounts only for the release of strained colloids, but the destruction of air-water interfaces during sand-pack imbibition probably contributed significantly to mobilization at pH 4.6, as these interfaces served as efficient collectors of kaolinite during the steady-flow stage of this experiment.

[30] The flow transients succeeded in mobilizing from 25 to 47% of the colloid mass retained within the columns. Maximum moisture contents measured during the transient stage equaled 0.2, which are well below the sand-pack porosity (0.34). Further increases in Θ would have undoubtedly mobilized more colloids, but such increases would have required exceedingly high flow rates. In natural vadose zone environments, clay-colloid mobilization is likely enhanced by perturbations in chemistry (e.g., reduction in ionic strength, increases in pH) that occur concomitantly with transients in flow. In an additional experiment, we found that 56% of kaolinite colloids trapped within a column under steady-flow conditions were mobilized during displacement of a pH-4.6 solution with a pH-7.4 solution. Although preliminary, these data suggest that chemical perturbations may, under some conditions, be of equal or of greater importance than flow perturbations in mobilizing clay colloids within the vadose zone.

[31] **Acknowledgments.** Department of Energy grants DE-FG07-02ER63492 (JES) and DE-FG07-02ER63491 (JNR) supported this research. Two anonymous reviewers provided constructive comments that led to improvement in the manuscript.

References

- Cherrey, K., M. Flury, and J. Harsh (2003), Nitrate and colloid transport through coarse Hanford sediments under steady state, variably saturated flow, *Water Resour. Res.*, 39(6), 1165, doi:10.1029/2002WR001944.
- Denovio, N., J. E. Saiers, and J. Ryan (2004), Colloid movement in unsaturated porous media: Recent advances and future directions, *Vadose Zone J.*, 3, 338–351.
- El-Farhan, Y. H., N. M. DeNovio, J. S. Herman, and G. M. Hornberger (2000), Mobilization and transport of soil particles during infiltration experiments in an agricultural field, Shenandoah Valley, Virginia, *Environ. Sci. Technol.*, 34, 3555–3559.
- Gamerding, A. P., and D. I. Kaplan (2001), Physical and chemical determinants of colloid transport and deposition in water-unsaturated sand and Yucca Mountain tuff material, *Environ. Sci. Technol.*, 35, 2497–2504.
- Langmuir, D. (1997), *Aqueous Environmental Chemistry*, Prentice-Hall, Old Tappan, N. J.
- Lenhart, J. J., and J. E. Saiers (2002), Transport of silica colloids through unsaturated porous media: Experimental results and model comparisons, *Environ. Sci. Technol.*, 36, 769–777.
- Pilgrim, D. H., and D. D. Huff (1983), Suspended sediment in rapid subsurface stormflow on a large field plot, *Earth Surf. Processes Landforms*, 8, 451–463.
- Rousseau, M., L. di Pietro, R. Angulo-Jaramillo, D. Tessier, and B. Cabibel (2004), Preferential transport of soil colloidal particles: Physicochemical effects on particle mobilization, *Vadose Zone J.*, 3, 247–261.
- Ryan, J. N., T. H. Illengasekare, M. I. Litaor, and R. Shannon (1998), Particle and plutonium mobilization in macroporous soils during rainfall simulations, *Environ. Sci. Technol.*, 32, 476–482.
- Saiers, J. E., and J. J. Lenhart (2002), Colloid mobilization and transport within unsaturated porous media under transient-flow conditions, *Water Resour. Res.*, 39(1), 1019, doi:10.1029/2002WR001370.
- Saiers, J. E., and J. J. Lenhart (2003), Ionic-strength effects on colloid transport and interfacial reactions in partially saturated porous media, *Water Resour. Res.*, 39(9), 1256, doi:10.1029/2002WR001887.
- Saiers, J. E., G. M. Hornberger, D. B. Gower, and J. S. Herman (2003), The role of moving air-water interfaces in colloid mobilization within the vadose zone, *Geophys. Res. Lett.*, 30(21), 2083, doi:10.1029/2003GL018418.
- Sparks, D. L. (1995), *Environmental Soil Chemistry*, 267 pp., Academic, San Diego, Calif.
- Sprague, L. A., J. S. Herman, G. M. Hornberger, and A. L. Mills (2000), Atrazine adsorption and colloid-facilitated transport through the unsaturated zone, *J. Environ. Qual.*, 29, 1632–1641.
- Wan, J., and T. K. Tokunaga (1997), Film straining of colloids in unsaturated porous media: Conceptual model and experimental testing, *Environ. Sci. Technol.*, 31, 2413–2420.
- Wan, J., and T. K. Tokunaga (2002), Partitioning of clay colloids at air-water interfaces, *J. Colloid Interface Sci.*, 247, 54–61.
- Wan, J., and J. L. Wilson (1994), Visualization of the role of the gas-water interface on the fate and transport of colloids in porous media, *Water Resour. Res.*, 30(1), 11–23.

B. Gao and J. E. Saiers, School of Forestry and Environmental Studies, Yale University, 205 Prospect Street, New Haven, CT 06511, USA. (james.saiers@yale.edu)

J. N. Ryan, Department of Civil, Environmental, and Architectural Engineering, University of Colorado, Boulder, CO 80309, USA.